Correlations between Mechanical and Electrical Properties of Polythiophenes

Brendan O'Connor,[†] Edwin P. Chan,[†] Calvin Chan,[†] Brad R. Conrad,[†] Lee J. Richter,[†] R. Joseph Kline,[†] Martin Heeney,[‡] Iain McCulloch,[‡] Christopher L. Soles,[†] and Dean M. DeLongchamp[†,*]

[†]National Institute of Standard and Technology, Gaithersburg, Maryland 20899, United States, and [‡]Imperial College London, London SW7 2AZ, U.K.

ABSTRACT The elastic moduli of polythiophenes, regioregular poly(3-hexylthiophene) (P3HT) and poly-(2,5-bis(3-alkylthiophene-2-yl)thieno[3,2-*b*]thiophene) (pBTTT), are compared to their field effect mobility showing a proportional trend. The elastic moduli of the films are measured using a buckling-based metrology, and the mobility is determined from the electrical characteristics of bottom contact thin film transistors. Moreover, the crack onset strain of pBTTT films is shown to be less than 2.5%, whereas that of P3HT is greater than 150%. These results show that increased long-range order in polythiophene semiconductors, which is generally thought to be essential for improved charge mobility, can also stiffen and enbrittle the film. This work highlights the critical role of quantitative mechanical property measurements in guiding the development of flexible organic semiconductors.

An advantage often attributed to organic semiconductors is the potential for flexible electronic devices,[1] which could be lightweight, conformal, storable by rolling or folding, and amenable to low-cost fabrication methods such as roll-to-roll processing. Achieving high performing flexible organic electronics is expected to significantly advance a range of technologies such as displays, solar power, imaging, and radio frequency identification tags. Flexible devices are typically composed of multiple layers having unique physical properties. Under flexure, differences in mechanical properties between the layers will result in a complex stress distribution that could lead to device failure. In addition, it has been suggested that the mechanical and electrical properties of the semiconductor may be correlated for some materials.[2] Thus, accurately characterizing the mechanical properties of these films and correlating their mechanical and electrical properties is critical in guiding the development of candidate materials for flexible applications.

Polythiophenes are a widely studied class of solution processable organic electronic materials which are of great interest for a range of devices such as thin film transistors (TFTs).[3] These polymers typically have alkyl side chains that aid solubility, allowing for solution processing, but also inhibit long-range order. Regioregular poly(3-hexylthiophene) (P3HT), one of the most extensively studied solution processable semiconductors, adopts a lamellar packing motif of conjugated backbones separated by alkyl side chain regions. The ring planes of P3HT orient "edge-on" upon the substrate such that the π-stacking direction is parallel to the substrate, giving rise to efficient two-dimensional charge transport appropriate for a TFT.[4] More recently, poly(2,5-bis(3-alkylthiophene-2-yl)thieno[3,2-*b*]thiophenes) (pBTTTs) have exhibited more ordered films with crystalline domains and higher charge carrier mobilities.[5] The improved performance of pBTTT is attributed to crystallization with three-dimensional order rather than two, resulting in larger crystal sizes and fewer defects. Generally, molecular crystals with strong interactions in all three dimensions have a high elastic modulus and are brittle, whereas those with more anisotropic intermolecular potentials (*e.g.*, strong interactions in some dimensions, weaker in others) tend to have a lower elastic modulus and are more ductile.[6] These considerations suggest that highly crystalline semiconducting polymers that provide high charge mobilities, such as pBTTT, will be stiffer and may be more likely to crack under strain. In this report, we show that indeed the improvement in field effect mobility of pBTTT over P3HT is correlated with an increase in

elastic modulus. Improving the molecular order of pBTTT *via* thermal annealing, which has been shown to further improve hole mobility,[7,8] also increases its elastic modulus. In addition, the strain level required for crack onset is discussed as a means of understanding when the polymer film will likely fail in a flexible device application, showing that the increase in elastic modulus correlates with brittle behavior.

RESULTS AND DISCUSSION

The elastic moduli of these films are characterized using a buckling-based metrology.[9] This approach is specifically designed to study thin films, which are difficult to measure with conventional mechanical testing methods. Briefly, the test film is initially spun cast onto a host substrate and then transferred to a second, relatively thick, prestrained soft elastic substrate. The tensile strain in the substrate is then released, applying compression to the top film. The modulus mismatch between the film and substrate results in a characteristic wrinkle pattern from which the mechanical properties of the film can be derived.[9] To systematically study the dependence of film thickness, the P3HT and pBTTT films are cast under varying solution concentrations and spin speeds. Details on film preparation can be found in the Materials and Methods. The cast films are then transferred to a slab of prestrained polydimethylsiloxane (PDMS), which is then released to generate compression.[10] Optical micrographs of P3HT and pBTTT films showing the typical buckling pattern are provided in Figure 1. The characteristic buckling wavelengths of P3HT and pBTTT films as-cast (AC) and thermally annealed at 180 °C (AN), for varying film thickness, are provided in Figure 2. The buckling wavelength was measured with either an optical microscope or an atomic force microscope (AFM), depending on the buckling wavelength. Note that varying the spin speed may affect the polymer film microstructure;[11] however, it does not appear to have a significant effect on the elastic modulus. The change in microstructural orientation by varying spin speed has also been shown to correlate with charge carrier mobility, and as will be shown below, there is not a large variation in the field effect mobility for the thick and thin films, suggesting a similar microstructure.[11] For thick pBTTT films (>60 nm), thermal annealing commonly results in film dewetting; however, minimal dewetting was observed for films reported in Figure 2 as observed by optical microscopy and measured with ellipsometry, supporting the consistency of the buckling wavelength trend with film thickness. It has also been shown that the mechanical properties of polymer thin films can be different compared to their bulk analogue when the film thickness is below 100 nm.[12] A thickness dependence was not observed for the films considered here, allowing a linear fit over the range of data in Figure 2. Thus, elastic modulus can
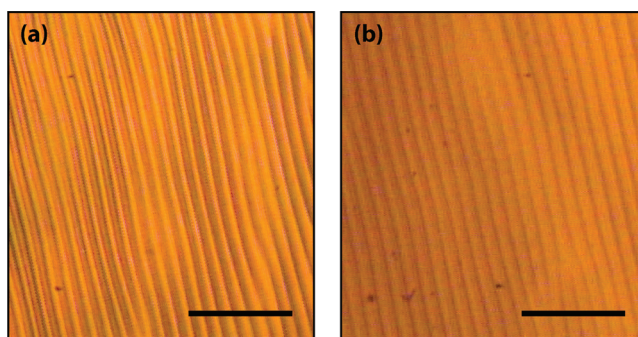

Figure 1. Optical micrographs of the buckling pattern observed for (a) P3HT film and (b) as-cast pBTTT film on PDMS under compression. The scale bar on the images is 100 μm.

be determined from the slope of the fit in Figure 2 and the relationship

$$\bar{E}_\mathrm{f} = 3\bar{E}_\mathrm{s}\left(\frac{\lambda_\mathrm{B}}{2\pi t}\right)^3 \qquad (1)$$

where, λ_B is the buckling wavelength, t is the film thickness, and the plain-strain modulus $\bar{E} = E(1 - \nu^2)$ where
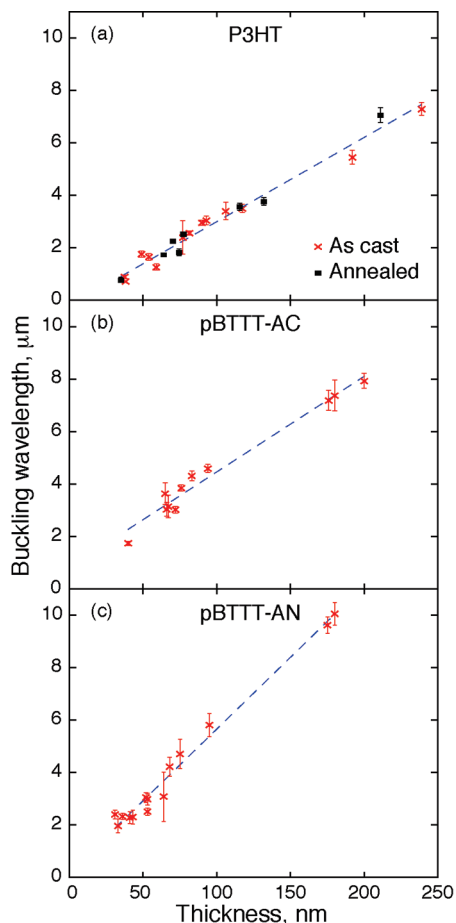

Figure 2. Characteristic buckling wavelength of films with varying thickness for (a) as-cast and annealed P3HT, (b) as-cast pBTTT-AC, and (c) annealed pBTTT-AN. The thermal treatment does not strongly affect the characteristic elastic modulus for P3HT, and the line fit is for both sets of data. Error bars at each thickness data point are based on one standard deviation of the measured buckling wavelength. The pooled standard deviation in measured film thickness is 1.5 nm.

v is the Possion ratio.[9] The elastic modulus of P3HT is determined to be $E_{P3HT} = 0.25 \pm 0.06$ GPa, the as-cast pBTTT is $E_{PBTTT-AC} = 0.9 \pm 0.2$ GPa, and the modulus of the thermally annealed pBTTT is $E_{PBTTT-AN} = 1.8 \pm 0.3$ GPa. The elastic modulus of PDMS, E_s, was between 0.6 and 0.75 MPa. The sample specific modulus of PDMS was measured for each cast batch from a tensile stress test, taking the slope of the stress−strain curve at strain levels applied during buckling measurements. In Figure 2, the buckling wavelengths are normalized to one elastic modulus of PDMS of 0.66 and 0.70 MPa for the P3HT and pBTTT plots, respectively. The Poisson ratio was assumed to be 0.5 and 0.35 for PDMS and the semiconducting polymers, respectively.[13] The elastic modulus of P3HT is lower than a previously reported value of 1.33 GPa using a similar measurement technique.[13] However, the elastic modulus of P3HT with comparable molecular weight is similar to previously reported values of bulk samples measured to be 0.08 GPa in a tensile test[14] and approximately 0.2 GPa by dynamic mechanical analysis.[15] It is important to emphasize that the technique reported here measures the in-plane elastic modulus, and the anisotropic microstructure of these films will likely lead to an anisotropic elastic modulus. However, for flexible device applications, strains will primarily be in the plane of the film and the in-plane modulus will dominate the mechanical response.

The observed difference in elastic modulus between P3HT and pBTTT films can be explained by considering how their microstructures differ. Because these films are semicrystalline, we must consider microstructure from two perspectives: (1) the molecular packing within crystals, and (2) the relative presence and arrangement (*e.g.*, shape, size, orientation) of crystals within the film. The characteristics of molecular packing will directly influence the modulus of individual crystals. The crystallinity and crystal arrangement will determine how the in-crystal modulus couples to the modulus of the whole film. Below we discuss how the molecular packing and crystallinity contribute to the differences in measured elastic modulus.

From a molecular packing perspective, a critical difference between P3HT and pBTTT is the behavior of the alkyl side chains in the room temperature crystal. In P3HT, the alkyl side chains are liquid-like and do not interdigitate, leading to poor vertical molecular registry in a cast film, shown schematically in Figure 3a.[16] On the other hand, the side chains of pBTTT do interdigitate, resulting in improved out-of-plane order and crystals that form in three dimensions (Figure 3b).[5] The interdigitated and crystalline nature of the alkyl side chains in pBTTT will likely inhibit molecular motion of the polymer backbone in the pBTTT film. The fused thiophene ring of pBTTT also has less conformational freedom compared to P3HT,[17] leading to a more rigid polymer backbone. These properties will likely result in a greater modulus for pBTTT over P3HT in the E_1 direction, illustrated in Figure 3. In the π-stacking direction (E_2), first principle calculations suggest a similar elastic modulus.[18] Combined, the in-crystal modulus in the E_1−E_2 plane will likely be higher in pBTTT but not large enough to account for the measured difference. Other features of the films must also contribute to the difference in elastic modulus.

The difference in molecular packing is thought to contribute to the greater level of crystallinity in pBTTT
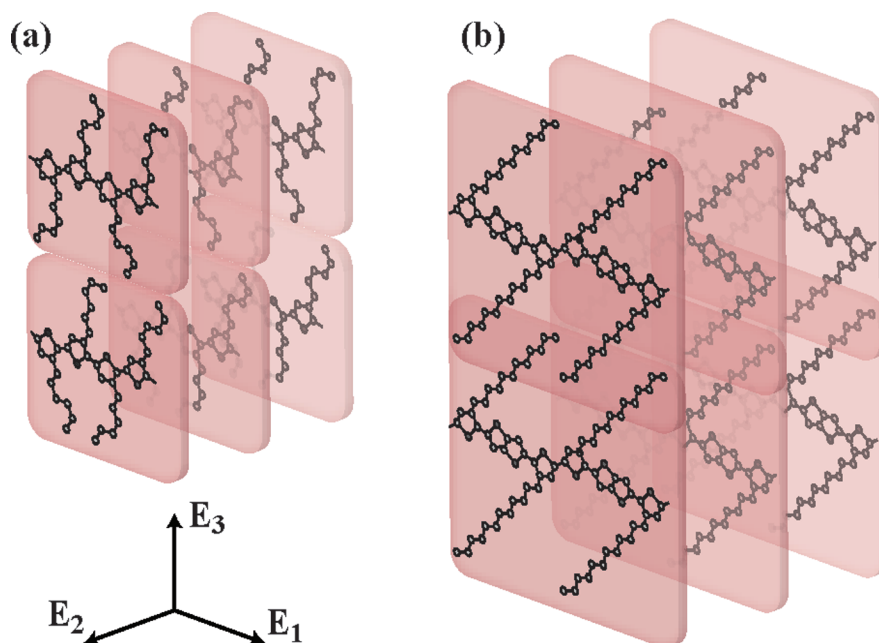

Figure 3. Schematic illustration of the widely accepted molecular packing geometry for the crystalline region of (a) P3HT and (b) pBTTT. In both films, this molecular packing is expected to result in an anisotropic elastic modulus within the crystalline region with $E_1 > E_2 > E_3$.

over P3HT,[5] a feature that will play a major role in the elastic modulus of the film. For thin films of these polymers prepared in a manner similar to or the same as our methods, the crystallinity of P3HT is thought to be ~50% or less,[19] whereas that of annealed pBTTT is thought to be greater than ~90%.[20] The level of crystallinity can strongly infuence the elastic modulus of a polymer film in two primary ways.[21] First, the crystalline regions will, in general, have a higher modulus than the amorphous regions due to improved molecular packing, increasing the density of intermolecular van der Waals bonds. Second, particularly for films near or above the glass transition temperature (T_g), crystalline regions can act similarly to cross-linkers and entanglements, tying segments of polymers chains together. The greater crystallinity of pBTTT over P3HT is therefore consistent with the greater elastic modulus of pBTTT films. We note that this conclusion requires the assumption that both polymers have a similar T_g and that any effects of relative molecular mass (aside from that on crystallinity) are relatively negligible.[21]

The origin of the elastic modulus difference between pBTTT-AC and pBTTT-AN requires more careful consideration. When the cast films are heated into the mesophase and cooled back to room temperature, the overall crystallinity increases slightly while the crystal size and orientation change substantially.[8,22] The increase in modulus upon annealing is consistent with the increased crystallinity, as we discussed above; however, it would likely be unable to account for the doubling in the elastic modulus that is observed. In addition to the level of crystallinity, the substantial change in modulus is more likely due to the increased size and reorientation of the crystals. Upon annealing, pBTTT has been shown to form larger crystalline domains within even larger monolayer terraces.[22] Increasing planar crystal size without changing the overall crystallinity has been shown to increase the modulus of semicrystalline polymers.[23] This can be explained by considering composite theory, discussed below in more detail. Along with the change in crystal size, there is also a reorientation of the plate-like pBTTT crystals, becoming more parallel to the substrate plane. Crystal reorientation alters the modulus due to the highly anisotropic molecular packing of pBTTT, as illustrated in Figure 3. For nearest neighbor molecules, the strength of the molecular orbital interaction of the conjugated backbone in the π-stacking direction is greater than the interaction between interdigitated alkyl side chains, leading to greater intermolecular bond strength in the π-stacking direction. This feature is reflected in infrared spectroscopy of pBTTT showing that at slightly elevated temperatures the side chains melt while π−π-stacking remains.[24] This difference in molecular interaction suggests that the modulus in the π-stacking direction (E_2) is greater than the modulus in the side-chain stacking direction (E_3), with vectors defined in Figure 3. The

modulus parallel to the chain itself (E_1) is likely the largest in the crystal because it would require substantial conformational changes to permit strain in this direction, which would necessarily disrupt packing in both the π-stacking and side-chain packing directions. The anisotropic in-crystal elastic modulus couples to the elastic modulus of the films in a manner that depends on crystal orientation. For the as-cast film, there is a substantial distribution of crystal orientations such that the crystalline contribution to in-plane film modulus should be a mixture of $E_1 - E_2$ (strong) with E_3 (weak).[8] In the annealed film, the crystals become more oriented such that $E_1 - E_2$ (strong) is essentially the only crystalline contribution to in-plane modulus and E_3 (weak) is confined to the out-of-plane direction.[8] Comparatively, the similarity in elastic moduli in annealed and as-cast P3HT films is consistent with their similar microstructures.[16]

To evaluate the relationship between the mechanical and charge transport properties of the films, bottom contact thin film transistors were fabricated. The device fabrication details are given in the Materials and Methods, and performance results are given in Table 1. We see that the mobility of pBTTT-AN is the highest followed by pBTTT-AC, then P3HT, as expected.[5] The mobility of each film is measured for two semiconductor thicknesses with little variation in performance observed. Annealed P3HT was not measured but is not expected to change substantially,[25,26] similar to the effect of annealing on the elastic modulus. The increase in mobility of pBTTT over P3HT has been attributed to improved crystal formation resulting in greater long-range order of the conjugated backbone.[5,22] Figure 4 compares the average mobility and the elastic modulus of these films, showing a proportional trend between films.

While large crystals do not necessarily improve charge mobility (as it does not for poly(9,9-di-*n*-octylfluorene-*alt*-benzothiadiazole), F8BT),[17] in general, for semicrystalline polymer semiconductors, improved carrier mobility is critically dependent on long-range order, which is aided by larger well-ordered crystals. Our results suggest that the increase in crystallinity, reduction in grain boundaries, and improved molecular order responsible for improved charge mobility is then reflected in an increase in the elastic modulus.[2,17] The role of crystallinity is further verified by considering the small molecule organic semiconductor pentacene. Pentacene has been shown to have field effect hole mobilities greater than 1.5 cm²/(V·s) when forming large crystalline domains.[27] This high charge mobility is consistent with pentacene's high elastic modulus of 16.09 GPa,[13] supporting the trend we report here. We would generally expect, however, that a modulus−mobility correlation would only hold *within* a family of chemically similar organic semiconductors

TABLE 1. Summary of the Mobility, Elastic Modulus, And Crack Onset Strain of the P3HT and pBTTT films[a]

film	P3HT		pBTTT-AC		pBTTT-AN	
thickness, nm	106	49	68	40	65	31
mobility, cm^2/(V · s)	0.06 ± 0.01	0.04 ± 0.01	0.08 ± 0.05	0.06 ± 0.01	0.32 ± 0.02	0.34 ± 0.01
elastic modulus, GPa	0.252 ± 0.057		0.879 ± 0.243		1.800 ± 0.345	
crack onset strain, %	>150		<2.5		<2.5	

[a]The pBTTT devices are measured under as-cast (AC) and annealed (AN) conditions. The reported elastic modulus of P3HT is for both as-cast and annealed films, and the mobility and the crack onset strain are for as-cast P3HT only. The crack onset strain is given for films on PDMS and strained in tension. Cracks were observed to consistently occur below 2.5% for the pBTTT films, while extremely large strains of over 150% have been applied to P3HT without the observation of crack formation. The error in mobility is based on one standard deviation of the devices tested. Error in the elastic modulus is based on standard error of the line fits given in Figure 2.

with similar conjugation length, intermolecular packing motif, and π-orbital overlap.

Determining the exact relationship between elastic modulus and charge carrier mobility is beyond the scope of this work. Qualitative consideration of models for the mechanical and electrical characteristics of semicrystalline polymers can provide insight into our observed trend. Charge transport models have been successfully developed that assign unique characteristics to high mobility intragranular transport and low mobility intergranular transport in semicrystalline organic electronics.[2] A simple model for mobility that considers only carriers randomly passing through the semicrystalline polymer is given as[2]

$$\mu = \frac{\mu_C \mu_M}{\mu_C(1 - V_C) + \mu_M V_C} \quad (2)$$

where μ_C is the charge mobility within a crystal, μ_M is the mobility within the amorphous material, and V_C is the volume fraction of crystalline material. Similarly, the elastic modulus of a semicrystalline polymer can be modeled as a composite of the higher crystalline modulus and lower amorphous modulus regions as[23]
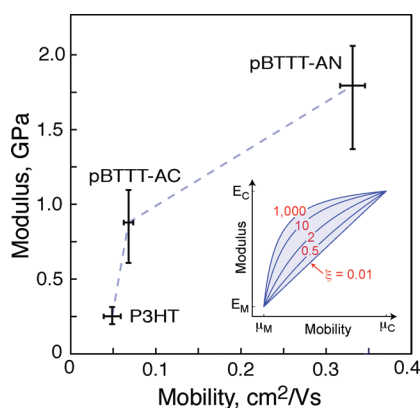

Figure 4. Comparison of the field effect mobility and elastic modulus of P3HT, as-cast pBTTT-AC, and annealed pBTTT-AN films. Further details on the values for field effect mobility, elastic modulus, and the error bars are given in Table 1. The dotted line is provided as a guide for the eye. Inset, the charge mobility and elastic modulus of a semicrystalline polymer with percent crystallinity. This trend is based on composite theories of charge transport and elastic modulus with two distinct values for the amorphous (μ_M, E_M) and crystalline (μ_C, E_C) portion of the film.

$$E = E_M \frac{1 + \xi\eta V_C}{1 - \eta V_C} \quad (3)$$

and

$$\eta = \frac{(E_C/E_M) - 1}{(E_C/E_M) + \xi} \quad (4)$$

where E_M is the modulus of the amorphous polymer, E_C is the modulus of the crystalline polymer, and ξ is a geometric parameter that for lamellae, representative of the polymers here, is equal to 2 times the length of the lamella divided by the height. On the basis of these models, the inset of Figure 4 shows trends for the charge mobility dependence on elastic modulus as the percent crystallinity of the film increases, given for a range of ξ. For quantitative comparison, critical details such as charge percolation effects and additional knowledge of crystal geometry are required; however, the models do provide mathematical framework that describes how the system depends on these details. For example, ξ could range from very small to greater than 20 and it could therefore play an important role in the correlation between elastic modulus and charge mobility. An increase in the lamellar geometric factor could increase the elastic modulus without requiring a large increase in crystallinity. This effect may contribute to the increase in elastic modulus upon annealing of pBTTT, which causes the lateral size of the lamellar crystals to increase substantially.

To consider the mechanical robustness of these films, we also determine the crack onset strain. Crack onset is critically important for these films if they are required to transport charge and expected to flex under operation. Crack formation will increase electrical resistivity for charge transport perpendicular to the crack direction.[28] To investigate the brittle behavior of the films, the crack onset strain is measured for each film on PDMS under an applied tensile strain. Here, the polymer thin film is transferred to PDMS and the composite is placed under uniaxial tension. Alternatively, for buckling measurements, while compression is applied to the PDMS substrate along one direction, a tensile strain develops in the transverse direction due to the Poisson effect. Optical micrographs for pBTTT films showing both buckling in the compressive direction
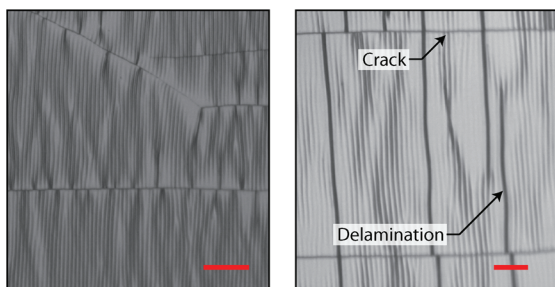
Figure 5. Optical micrographs of the characteristic crack formation in pBTTT films. The buckling pattern of the film under compression is observed, while the transverse direction is put in tension resulting in the onset of cracks. Once cracks form, the film begins to delaminate in the buckled direction. For both micrographs the scale bar is 50 μm.

and crack formation in the tensile direction are shown in Figure 5. Under tension, the crack onset strain for pBTTT is found to be below 2.5% for both the as-cast and thermally annealed films. The strain levels are too low to obtain higher levels of precision using the current optical microscopy testing methodology; therefore, differences in the crack onset strain for annealed and as-cast films were not observed.[29] In stark contrast to the pBTTT, P3HT films allow for strains over 150%, plastically deforming without crack formation. The behavior of pBTTT can in part be attributed to the isotropic in-plane crystalline distribution, a characteristic that tends to cause brittleness in semicrystalline polymers with low strength.[21] In addition, while interdigitation of pBTTT side chains inhibits molecular motion, the lack of registration in P3HT crystals and the conformational disorder of its side chains likely permit the more ductile behavior. We note that crack formation will have a substrate dependence;[30] however, the elastic substrate is suitable for comparison purposes. For device applications, the details of the device structure must be known and may alter the strain in which cracks develop.

CONCLUSION

We have measured the elastic modulus for P3HT, which is moderately crystalline, and pBTTT, which is highly crystalline. We show that for thermally annealed pBTTT the elastic modulus is ~7.1 times greater than the modulus of P3HT, very similar to the hole mobility ratio of ~6.8. In addition, we find that the crack onset strain of pBTTT films is less than 2.5%, whereas that of P3HT films is greater than 150%. These results expand upon the complex role of side chains in the properties of thiophene polymers: their solubility aids processing, their interdigitation can provide a mechanism to grow and repair large crystals, and the details of their packing interactions can lead to films that are either flexible and ductile or stiff and brittle.

Quantitative measurements of elastic modulus in semiconductor films are important in the design of multilayer devices intended to undergo flexure. Under flexure, significant differences in modulus between adjacent layers (e.g., semiconductor and dielectric) will result in complex stress distributions that must be accommodated to avoid device delamination by adhesive or cohesive failure. For any flexible device application, brittle films are clearly undesirable. The crack onset strain of pBTTT is similar to that of indium tin oxide, which is thought to be undesirable in flexible electronics, with alternatives actively being sought.[31,32] This report emphasizes that consideration of mechanical properties should be a critical element in the development of new semiconducting polymers and fabrication processes for flexible device applications.

MATERIALS AND METHODS

Materials. The P3HT was obtained from Plextronics Inc. with a number-average molecular mass $M_n = 62$ kD, a regioregularity of 99%, and a polydispersion of 1.9 measured by gel permeation chromatography (GPC). The pBTTT was synthesized following a previously described process,[3] with alkyl side chains consisting of $C_{12}H_{25}$, a number average molar mass $M_n = 29$ kD, and a polydispersion of 1.9.

Film Preparation. P3HT is dissolved into chloroform at 6 to 10 mg/mL. The pBTTT is dissolved in a combination of 1,2-dichlorobenze and chloroform at a volume ratio between 6:1 and 8:1 and a concentration ranging from 4 to 8 mg/mL. The P3HT solution is cast at room temperature, while the pBTTT solution is cast warm (30−50 °C), both at spinning rates between (750(2π) and 3000(2π)) rad/min (i.e., 750 and 3000 rpm) onto octyltrichlorosilane (OTS)-treated silicon substrates with either a native or 200 nm thermal oxide layer. After spin-casting, a portion of the samples are left as-cast (designated AC), while the other samples (designated AN) are heated to 180 °C for 5 min and cooled slowly back to room temperature at approximately 10 °C/min.[3] The OTS self-assembled monolayer was formed by a previously described process.[8] The thickness of the cast films is measured using spectroscopic ellipsometry using an anisotropic model dielectric function as described previously.[33]

Characterization. The bottom contact transistors consist of a 300 nm SiO_2 gate dielectric on a highly doped p-type Si wafer and 50 nm Pt source and drain electrodes. The channel width is 1 mm, while the channel length varied from 10 to 100 μm. There was not a large channel length dependence observed; however, the reported results are for the 10 μm channel length devices. The transistors were measured using Keithly 6430 SourceMeters. The TFTs where measured in the saturated regime by sweeping the gate voltage (V_g) from −25 to 80 V, with a source−drain voltage of 90 V. The field effect hole mobilities were calculated from a linear fit of $I_{sd}^{1/2}$ versus V_g, where I_{sd} is the source−drain current.

For buckling measurements, the reported buckling wavelength is based on counting the number of buckles in a row of set length and then dividing that length by the number counted. This is done repeatedly for a given film and averaged to get the characteristic wavelength. The polydimethylsiloxane (PDMS) substrate used for buckling and crack onset analysis was ~2 mm thick, cast with a cross-linker concentration of 10:1, and cured at a temperature of 50 °C for over 12 h. The elastic modulus of PDMS is measured by a tensile test procedure using a texture ananlyzer (Texture Technologies TX.XT2i) and varied between 0.6 and 0.75 MPa depending on the batch.

All polymer processing was performed in a nitrogen environment, ellipsometric and strain measurements were completed

in atmosphere, and transistor device testing was performed under a nitrogen purged environment. All experiments were conducted at room temperature.

REFERENCES AND NOTES

1. Forrest, S. R. The Path to Ubiquitous and Low-Cost Organic Electronic Appliances on Plastic. *Nature* **2004**, *428*, 911–918.

2. Street, R. A.; Northrup, J. E.; Salleo, A. Transport in Polycrystalline Polymer Thin-Film Transistors. *Phys. Rev. B* **2005**, *71*, 165202.

3. McCulloch, I.; Heeney, M.; Bailey, C.; Genevicius, K.; Macdonald, I.; Shkunov, M.; Sparrowe, D.; Tierney, S.; Wagner, R.; Zhang, W. M.; *et al.* Liquid-Crystalline Semiconducting Polymers with High Charge-Carrier Mobility. *Nat. Mater.* **2006**, *5*, 328–333.

4. Sirringhaus, H.; Brown, P. J.; Friend, R. H.; Nielsen, M. M.; Bechgaard, K.; Langeveld-Voss, B. M. W.; Spiering, A. J. H.; Janssen, R. A. J.; Meijer, E. W.; Herwig, P.; *et al.* Two-Dimensional Charge Transport in Self-Organized, High-Mobility Conjugated Polymers. *Nature* **1999**, *401*, 685–688.

5. Kline, R. J.; DeLongchamp, D. M.; Fischer, D. A.; Lin, E. K.; Richter, L. J.; Chabinyc, M. L.; Toney, M. F.; Heeney, M.; McCulloch, I. Critical Role of Side-Chain Attachment Density on the Order and Device Performance of Polythiophenes. *Macromolecules* **2007**, *40*, 7960–7965.

6. Reddy, C. M.; Padmanabhan, K. A.; Desiraju, G. R. Structure−Property Correlations in Bending and Brittle Organic Crystals. *Cryst. Growth Des.* **2006**, *6*, 2720–2731.

7. Chabinyc, M. L.; Toney, M. F.; Kline, R. J.; McCulloch, I.; Heeney, M. X-ray Scattering Study of Thin Films of Poly(2,5-bis(3-alkylthiophen-2-yl)thieno[3,2-*b*]thiophene). *J. Am. Chem. Soc.* **2007**, *129*, 3226–3237.

8. Kline, R. J.; DeLongchamp, D. M.; Fischer, D. A.; Lin, E. K.; Heeney, M.; McCulloch, I.; Toney, M. F. Significant Dependence of Morphology and Charge Carrier Mobility on Substrate Surface Chemistry in High Performance Polythiophene Semiconductor Films. *App. Phys. Lett.* **2007**, 90.

9. Stafford, C. M.; Harrison, C.; Beers, K. L.; Karim, A.; Amis, E. J.; Vanlandingham, M. R.; Kim, H. C.; Volksen, W.; Miller, R. D.; Simonyi, E. E. A Buckling-Based Metrology for Measuring the Elastic Moduli of Polymeric Thin Films. *Nat. Mater.* **2004**, *3*, 545–550.

10. Stafford, C. M.; Guo, S.; Harrison, C.; Chiang, M. Y. M. Combinatorial and High-Throughput Measurements of the Modulus of Thin Polymer Films. *Rev. Sci. Instrum.* **2005**, 76.

11. DeLongchamp, D. M.; Vogel, B. M.; Jung, Y.; Gurau, M. C.; Richter, C. A.; Kirillov, O. A.; Obrzut, J.; Fischer, D. A.; Sambasivan, S.; Richter, L. J.; *et al.* Variations in Semiconducting Polymer Microstructure and Hole Mobility with Spin-Coating Speed. *Chem. Mater.* **2005**, *17*, 5610–5612.

12. Stafford, C. M.; Vogt, B. D.; Harrison, C.; Julthongpiput, D.; Huang, R. Elastic Moduli of Ultrathin Amorphous Polymer Films. *Macromolecules* **2006**, *39*, 5095–5099.

13. Tahk, D.; Lee, H. H.; Khang, D. Y. Elastic Moduli of Organic Electronic Materials by the Buckling Method. *Macromolecules* **2009**, *42*, 7079–7083.

14. Muller, C.; Goffri, S.; Breiby, D. W.; Andreasen, J. W.; Chanzy, H. D.; Janssen, R. A. J.; Nielsen, M. M.; Radano, C. P.; Sirringhaus, H.; Smith, P.; *et al.* Tough, Semiconducting Polyethylene-Poly(3-hexylthiophene) Diblock Copolymers. *Adv. Funct. Mater.* **2007**, *17*, 2674–2679.

15. Kuila, B. K.; Nandi, A. K. Physical, Mechanical, and Conductivity Properties of Poly(3-hexylthiophene)-Montmorillonite Clay Nanocomposites Produced by the Solvent Casting Method. *Macromolecules* **2004**, *37*, 8577–8584.

16. Gurau, M. C.; Delongchamp, D. M.; Vogel, B. M.; Lin, E. K.; Fischer, D. A.; Sambasivan, S.; Richter, L. J. Measuring Molecular Order in Poly(3-alkylthiophene) Thin Films with Polarizing Spectroscopies. *Langmuir* **2007**, *23*, 834–842.

17. Chabinyc, M. L.; Jimison, L. H.; Rivnay, J.; Salleo, A. Connecting Electrical and Molecular Properties of Semiconducting Polymers for Thin-Film Transistors. *MRS Bull.* **2008**, *33*, 683–689.

18. Northrup, J. E. Atomic and Electronic Structure of Polymer Organic Semiconductors: P3HT, PQT, and PBTTT. *Phys. Rev. B* **2007**, 76.

19. Wu, Z. Y.; Petzold, A.; Henze, T.; Thurn-Albrecht, T.; Lohwasser, R. H.; Sommer, M.; Thelakkat, M. Temperature and Molecular Weight Dependent Hierarchical Equilibrium Structures in Semiconducting Poly(3-hexylthiophene). *Macromolecules* , *43*, 4646–4653.

20. DeLongchamp, D. M.; Kline, R. J.; Lin, E. K.; Fischer, D. A.; Richter, L. J.; Lucas, L. A.; Heeney, M.; McCulloch, I.; Northrup, J. E. High Carrier Mobility Polythiophene Thin Films: Structure Determination by Experiment and Theory. *Adv. Mater.* **2007**, *19*, 833–937.

21. Nielsen, L. E.; Landel, R. F. *Mechanical Propertied of Polymers and Composites*, 2nd ed.; Marcel Dekker: New York, 1994.

22. Wang, C. C.; Jimison, L. H.; Goris, L.; McCulloch, I.; Heeney, M.; Ziegler, A.; Salleo, A. Microstructural Origin of High Mobility in High-Performance Poly(thieno-thiophene) Thin-Film Transistors. *Adv. Mater.* **2010**, *22*, 697–701.

23. Andrews, E. H. Morphology and Mechanical-Properties in Semicrystalline Polymers. *Pure Appl. Chem.* **1974**, *39*, 179–194.

24. DeLongchamp, D. M.; Kline, R. J.; Jung, Y.; Lin, E. K.; Fischer, D. A.; Gundlach, D. J.; Cotts, S. K.; Moad, A. J.; Richter, L. J.; Toney, M. F.; *et al.* Molecular Basis of Mesophase Ordering in a Thiophene-Based Copolymer. *Macromolecules* **2008**, *41*, 5709–5715.

25. Surin, M.; Leclere, P.; Lazzaroni, R.; Yuen, J. D.; Wang, G.; Moses, D.; Heeger, A. J.; Cho, S.; Lee, K. Relationship between the Microscopic Morphology and the Charge Transport Properties in Poly(3-hexylthiophene) Field-Effect Transistors. *J. Appl. Phys.* **2006**, 100.

26. Cho, S.; Lee, K.; Yuen, J.; Wang, G. M.; Moses, D.; Heeger, A. J.; Surin, M.; Lazzaroni, R. Thermal Annealing-Induced Enhancement of the Field-Effect Mobility of Regioregular Poly(3-hexylthiophene) Films. *J. Appl. Phys.* **2006**, 100.

27. Lin, Y. Y.; Gundlach, D. J.; Nelson, S. F.; Jackson, T. N. Stacked Pentacene Layer Organic Thin-Film Transistors with Improved Characteristics. *IEEE Electron Device Lett.* **1997**, *18*, 606–608.

28. Cairns, D. R.; Witte, R. P.; Sparacin, D. K.; Sachsman, S. M.; Paine, D. C.; Crawford, G. P.; Newton, R. R. Strain-Dependent Electrical Resistance of Tin-Doped Indium Oxide on Polymer Substrates. *Appl. Phys. Lett.* **2000**, *76*, 1425–1427.

29. Leterrier, Y.; Medico, L.; Demarco, F.; Manson, J. A. E.; Betz, U.; Escola, M. F.; Olsson, M. K.; Atamny, F. Mechanical Integrity of Transparent Conductive Oxide Films for Flexible Polymer-Based Displays. *Thin Solid Films* **2004**, *460*, 156–166.

30. Ye, T.; Suo, Z.; Evans, A. G. Thin-Film Cracking and the Roles of Substrate and Interface. *Int. J. Solids Struct.* **1992**, *29*, 2639–2648.

31. O'Connor, B.; Haughn, C.; An, K. H.; Pipe, K. P.; Shtein, M. Transparent and Conductive Electrodes Based on Unpatterned, Thin Metal Films. *Appl. Phys. Lett.* **2008**, 93.

32. Lee, J. Y.; Connor, S. T.; Cui, Y.; Peumans, P. Solution-Processed Metal Nanowire Mesh Transparent Electrodes. *Nano Lett.* **2008**, *8*, 689–692.

33. Delongchamp, D. M.; Kline, R. J.; Fischer, D. A.; Richter, L. J.; Toney, M. F. Molecular Characterization of Organic Electronic Films. *Adv. Mater.* In press.